

Electronic properties of single-crystalline $\text{Fe}_{1.05}\text{Te}$ and $\text{Fe}_{1.03}\text{Se}_{0.30}\text{Te}_{0.70}$

G. F. Chen, Z. G. Chen, J. Dong, W. Z. Hu, G. Li, X. D. Zhang, P. Zheng, J. L. Luo, and N. L. Wang
*Beijing National Laboratory for Condensed Matter Physics, Institute of Physics, Chinese Academy of Sciences,
 Beijing 100190, People's Republic of China*

(Received 7 April 2009; published 28 April 2009)

We report on a comprehensive study of the transport, specific heat, magnetic susceptibility, and optical spectroscopy on single crystal of $\text{Fe}_{1.05}\text{Te}$, which undergoes a first-order phase transition near 65 K. We show that its physical properties are considerably different from other parent compounds of FeAs-based systems, presumably attributed to the presence of excess Fe ions. The charge transport is rather incoherent above the transition, and no clear signature of the gap is observed below the transition temperature. Strong impurity scattering effect exists also in Se-doped superconducting sample $\text{Fe}_{1.03}\text{Se}_{0.30}\text{Te}_{0.70}$, leading to a relatively low T_c but a rather high upper critical field.

DOI: 10.1103/PhysRevB.79.140509

PACS number(s): 74.70.-b, 74.25.Gz, 74.25.Fy

The recent discovery of superconductivity in Fe- and Ni-based transition metal oxypnictides has triggered tremendous interest in searching for new Fe-based superconductors with similar PbO-type tetrahedral layers.¹ FeSe(Te) belongs to this tetragonal family with the simplest crystal structure. It comprises only a continuous stacking of tetrahedral FeSe(Te) layers along the c axis. Superconductivity with transition temperature T_c up to 15 K was obtained on $\text{Fe}_{1+x}(\text{Se},\text{Te})$ system at ambient pressure.²⁻⁴ The T_c can go up to 27 K at a pressure of 1.48 GPa.⁵ First-principles calculations⁶ on stoichiometric FeSe indicate that the electron-phonon coupling cannot explain the superconductivity at such a high transition temperature, and FeSe is in the category of unconventional superconductivity. The calculated Fermi surface (FS) structures of FeS, FeSe, and FeTe are very similar to that of FeAs-based superconductors, with cylindrical hole sections at the zone center and electron sections at the zone corner. Those Fermi surfaces are separated by a two-dimensional nesting wave vector at (π, π) . Spin-density-wave (SDW) ground state is obtained due to the substantial FS nesting effect. In particular, in going from FeSe to FeTe, the strength of the SDW instability is strongly enhanced.

Experimentally, it is difficult to synthesize the stoichiometric FeSe(Te), and excess Fe is always present in synthesized compounds.^{2-4,7-9} Those excess Fe ions occupy randomly on the Fe(2) sites as in Fe_2As compound or the Li sites in LiFeAs compound (both have Cu_2Sb type structure).⁸⁻¹¹ The superconductivity was found to appear in wide range of compositions $\text{Fe}_{1+y}\text{Se}_x\text{Te}_{1-x}$ ($0 < x \leq 1$),^{3,4} but the Se-free Fe_{1+y}Te undergoes a structural distortion along with the establishment of a long-range SDW order near 65 K.⁷⁻⁹ This is consistent with the expectation of the first-principles density-functional calculation showing higher strength of SDW instability for FeTe.⁶ However, a complex incommensurate long-range antiferromagnetic (AF) order is formed.⁸ With the reduction in the excess Fe, the AF order tends to be commensurate, but the moments rotate 45° relative to the moment direction found in other FeAs-based AF spin structures [along the orthorhombic long (a) axis].^{8,9} More recent density-functional calculations¹¹ indicate that the excess Fe is in a valence state near Fe^+ and therefore donates electron to the system. Furthermore, the excess Fe has a large magnetic moment and interacts with the magnetism of FeTe layers, resulting in a complex magnetic order.

Due to the interaction of the magnetic moment of excess Fe with the itinerant electrons of FeTe layer, we can expect that the electronic properties would be substantially affected. It is of great interest to investigate the electronic properties of this material and compare them with LaFeAsO and AFe_2As_2 ($A = \text{Ba}, \text{Sr}$) systems. Here we report on a comprehensive study of the transport, specific heat, magnetic susceptibility, and optical spectroscopy on single crystals of $\text{Fe}_{1.05}\text{Te}$ and $\text{Fe}_{1.03}\text{Se}_{0.30}\text{Te}_{0.70}$. We confirm that $\text{Fe}_{1.05}\text{Te}$ undergoes a first-order phase transition near 65 K. Above T_{SDW} , dc resistivity shows a nonmetallic behavior. In accord with this property, the optical conductivity displays a rather flat spectral line shape with an absence of Drude component. This suggests that there is almost no well-defined quasiparticle with sufficiently long lifetime. Below T_{SDW} , a small Drude weight develops at low frequency, reflecting a dramatic reduction in carrier scattering rate. But unlike LaFeAsO and SrFe_2As_2 , there is no clear sign of gap opening from optical, Hall coefficient, and low- T specific-heat measurement results. This is compatible with the disappearance of commensurate SDW caused by the size mismatch between the electron and hole Fermi surfaces induced by excess Fe as suggested by recent density-functional calculations.¹¹ The present work provides strong evidence that the excess Fe moments strongly scatter the charge carriers in FeAs layers. The superconducting properties of a $\text{Fe}_{1.03}\text{Se}_{0.30}\text{Te}_{0.70}$ single crystal are also investigated. A surprisingly high upper critical field is observed, again yielding evidence for strong impurity scattering effect in the superconducting sample.

Large single crystals of $\text{Fe}_{1.05}\text{Te}$ and $\text{Fe}_{1.03}\text{Se}_{0.30}\text{Te}_{0.70}$ have been grown by the Bridgeman technique. The starting compositions were selected as FeTe and $\text{FeSe}_{0.30}\text{Te}_{0.70}$, respectively. The mixtures of Fe and Te(Se) were grounded thoroughly and sealed in an evacuated quartz tube. The tube was heated at 920°C and cooled down slowly ($4^\circ\text{C}/\text{h}$) to grow single crystals. The obtained crystals were checked by x-ray diffraction (XRD) and their compositions were determined by inductively coupled plasma (ICP) analysis. The resistivity was measured by the standard four-probe method. The dc magnetic susceptibility was measured with a magnetic field of 1 T. The Hall coefficient measurement was done using a five-probe technique. The specific-heat measurement was carried out using a thermal relaxation calorimeter. Those measurements were performed down to 1.8 K in

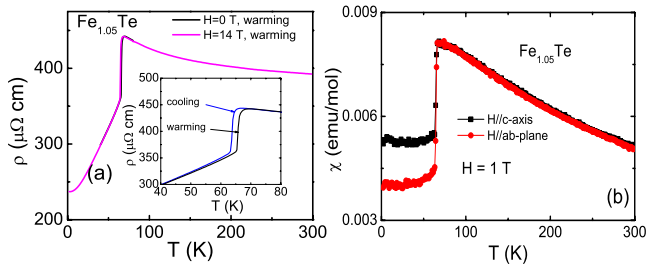


FIG. 1. (Color online) (a) The in-plane resistivity ρ_{ab} for $\text{Fe}_{1.05}\text{Te}$ in zero field and 14 T with $H\parallel c$ axis, respectively. (b) Magnetic susceptibility of $\text{Fe}_{1.05}\text{Te}$ as a function of temperature with $H\parallel ab$ plane and $H\parallel c$ axis, respectively.

a physical property measurement system (PPMS) of Quantum Design Co. The optical reflectance measurements were performed on Bruker IFS 66 v/s spectrometer on newly cleaved surfaces (ab plane) of those crystals up to $25\,000\text{ cm}^{-1}$. An *in situ* gold and aluminum overcoating technique was used to get the reflectivity $R(\omega)$.¹² The real part of conductivity $\sigma_1(\omega)$ is obtained by the Kramers-Kronig transformation of $R(\omega)$.

Figure 1(a) shows the temperature dependence of in-plane resistivity ρ_{ab} of $\text{Fe}_{1.05}\text{Te}$ in zero field and 14 T (magnetic field along the c axis). At high temperature, the resistivity shows a semiconductorlike behavior; i.e., ρ_{ab} increases slowly with decreasing temperature, whereas ρ_{ab} drops steeply below 65 K and then behaves quite metallic. This discontinuous change in the resistivity at 65 K is due to a structural phase transition, accompanied by magnetic transition.^{8,9} A thermal hysteresis of 2 K is clearly seen in the inset of Fig. 1(a). The resistivity data were measured at a slow heating and cooling rate of 3 K/min. This is consistent with the recent neutron-diffraction measurements on Fe_{1+y}Te polycrystalline samples, which indicated that the $P4/nmm$ tetragonal structure distorts to a $Pmnm$ orthorhombic⁸ or a $P2_1/m$ monoclinic structure⁹ and $\text{Fe}_{1.05}\text{Te}$ orders into an incommensurate magnetic state when the temperature is lowered below ~ 65 K. We have also attempted to probe the influence of magnetic fields on the $\rho(T)$ behavior. We find that the magnetic transition temperature is insensitive to the applied field and the magnetoresistance is negligibly small in the AF state (less than 0.5% near 2 K at the maximum applied field of 14 T). This behavior is different from that observed in SrFe_2As_2 , $[\rho_{ab}(8T) - \rho_{ab}(0T)]/\rho_{ab}(0T)$ reaching as high as 20% at 10 K.¹³ This indicates that the magnetic coupling is much stronger in FeTe compared to other FeAs-based systems.

In Fig. 1(b), we present the temperature dependence of magnetic susceptibility χ in a field of 1 T with $H\parallel ab$ and $H\parallel c$ axis, respectively. Near 65 K, χ decreases abruptly by a factor of 2, indicative of the presence of the first-order phase transition. Above this temperature, χ shows a Curie-Weiss-type behavior: χ decreases with increasing T . This is in contrast to those observed in $R\text{FeAsO}$ ($R=\text{La}$ and rare-earth elements) and $A\text{Fe}_2\text{As}_2$ ($A=\text{Sr}, \text{Ba}$) parent compounds above T_{SDW} .^{1,13,14} The behavior could thus be attributed to the excess Fe with local moment formation. Nevertheless, a simple Curie-Weiss law could not reproduce the experimental data

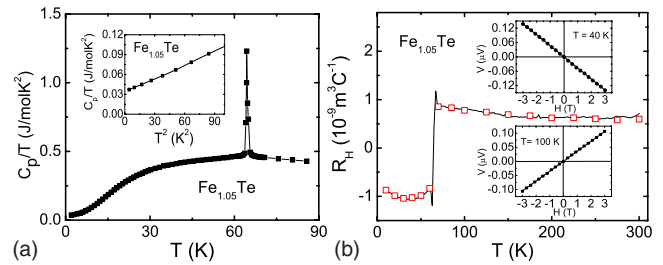


FIG. 2. (Color online) (a) Temperature dependence of specific-heat C for $\text{Fe}_{1.05}\text{Te}$. Inset: T^2 dependence of C/T in low temperatures. (b) Temperature dependence of Hall coefficient for $\text{Fe}_{1.05}\text{Te}$. The insets show the transverse voltage as a function of applied magnetic field measured at $T=40$ and 100 K, respectively.

well, which could be ascribed to the short-range antiferromagnetic correlation or spin fluctuation of FeTe layers.

To get more information about the magnetic and structural phase transition, we performed specific-heat measurement for $\text{Fe}_{1.05}\text{Te}$. Figure 2(a) shows the temperature dependence of specific heat C_p from 2 to 90 K. We can see clearly a sharp δ -function shape peak at about 65 K with $\Delta C \sim 0.8\text{ J/mol K}$. This is a characteristic feature of a first-order phase transition; even though the relaxation method employed in PPMS to measure heat capacity suppresses sharp features due to first-order transitions. The transition temperature agrees well with that observed in resistivity and magnetic susceptibility measurements. It is worth noting that only one peak at around 65 K is observed in $\text{Fe}_{1.05}\text{Te}$. This suggests that the structural transition and magnetic order occur at the same temperature. A number of studies suggested that the structural phase transition is driven by the magnetic transition. Depending on the strength of coupling along the c axis, the structural and magnetic transitions could occur simultaneously or separately.¹⁵ On this basis, the FeTe compound may have a strong interlayer coupling. At low temperatures, a good linear T^2 dependence of C_p/T is observed, indicating that the specific heat C_p is mainly contributed by electrons and phonons [see inset of Fig. 2(a)]. The fit yields the electronic coefficient $\gamma=34\text{ mJ/mol K}^2$ and the Debye temperature $\theta_D=141\text{ K}$. The electronic coefficient is significantly larger than the values obtained from the band structure calculations.¹⁶ Note that, for the parent compound of LaFeAsO and SrFe_2As_2 , the electronic coefficients are significantly smaller than the values obtained from the band structure calculations for nonmagnetic state. It was explained as due to a partial energy gap opening below SDW transition which removes parts of the density of states.^{13,17} Thus, the higher value here suggests an absence of gap opening below the transition.

Figure 2(b) shows the Hall coefficient data between 10 and 300 K for $\text{Fe}_{1.05}\text{Te}$. The inset shows the verification of the Hall voltage driven by magnetic field where a linear dependence of the transverse voltage on the applied magnetic field is observed up to 3 T at 100 K. Two sets of data were presented in the main panel. The empty squares are Hall coefficient data measured by scanning magnetic field at fixed temperature, while the solid black curve is R_H determined from two separate temperature scans under fixed applied

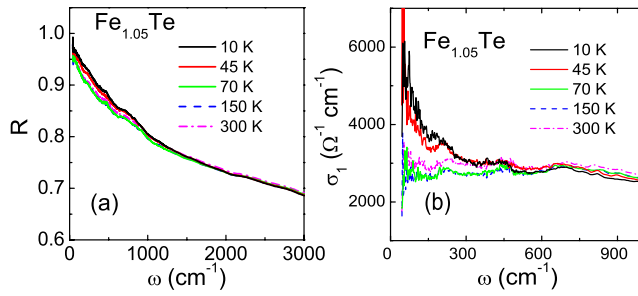


FIG. 3. (Color online) (a) Optical reflectance and (b) conductivity spectra at different temperatures for $\text{Fe}_{1.05}\text{Te}$.

magnetic field at 3 T, respectively. They show a rather good match. In Fig. 2(b), we find that there is an abrupt sign change in R_H at 65 K, but the absolute values are almost unchanged. Furthermore, R_H in $\text{Fe}_{1.05}\text{Te}$ is nearly temperature independent even below 65 K. Those behaviors are considerably different from the FeAs -based parent compounds. For example, in the case of SrFe_2As_2 , R_H drops quickly below T_{SDW} and continuously decreases to a very large negative value with decreasing temperature. The absolute value of R_H at 2 K is about 35 times larger than that above T_{SDW} .¹³ The huge increase in the R_H value is naturally explained by the gapping/reconstruction of the FS in the magnetic ordered phase. This was indeed confirmed by the optical spectroscopy measurement.¹⁸ Here, R_H only shows an abrupt sign change but keeps almost the same absolute value. This may again indicate that the FS is not gapped. The change might be caused only by a sudden reconstruction of band structure. Further effort on this issue is still needed.

To further probe the carrier dynamics, we measured the optical response of the $\text{Fe}_{1.05}\text{Te}$ crystal. Figure 3 shows the reflectance $R(\omega)$ and conductivity $\sigma_1(\omega)$ spectra at different temperatures. In accord with the nonmetallic dc resistivity above T_{SDW} , we find that the low-frequency reflectance decreases slightly with decreasing temperature from 300 to 70 K, leading to a reduction in low- ω conductivity. It is important to note that the conductivity spectra above T_{SDW} are rather flat. Clearly, it is not a semiconductor as $\sigma_1(\omega)$ does not indicate the presence of a semiconductorlike gap, but it is not a usual metal as well because of the absence of a Drude-type peak. As is well known, the width of Drude peak is linked with the scattering rate (or inverse of the transport lifetime) of the quasiparticle; the measurement result indicates that there is no well-defined quasiparticle with sufficiently long transport lifetime above T_{SDW} . This means that the charge transport is rather incoherent. Below T_{SDW} , the low- ω $R(\omega)$ increases fast. Correspondingly, a Drude component in $\sigma_1(\omega)$ develops at low frequency, reflecting a dramatic reduction of the carrier scattering rate in the magnetic ordered state. However, unlike the parent compounds of LaFeAsO and AFe_2As_2 ($A=\text{Ba}, \text{Sr}$), there is no partial gap formation in optical spectra below T_{SDW} , which is consistent with the specific-heat and Hall coefficient data mentioned above.

All above experiment results indicate that the $\text{Fe}_{1.05}\text{Te}$ compound is very different from the LaFeAsO and AFe_2As_2 ($A=\text{Ba}, \text{Sr}$) parent compounds. In LaFeAsO and AFe_2As_2

($A=\text{Ba}, \text{Sr}$), the charge carriers are itinerant and the SDW order is driven by the nesting of FS, which also leads to a partial energy gap formation and a removal of a large part of conducting carriers. However, in $\text{Fe}_{1.05}\text{Te}$, no well-defined quasiparticles with sufficiently long lifetime exist above T_{SDW} , very likely due to strong magnetic scattering from the excess Fe ions, and furthermore, no clear gap formation is seen below T_{SDW} . Those behaviors might be understood from a local moment picture with complex frustrations,^{16,19} but recent density-functional calculations based on itinerant framework indicate that the doping effect and the large magnetic moment induced by excess Fe could cause a size mismatch between the electron and hole Fermi surfaces and a disappearance of commensurate SDW order.¹¹ The cooperative effect of excess Fe and the electrons in the FeTe layers may give such complicated behavior.

Finally we present the physical properties of a superconducting single crystal $\text{Fe}_{1.03}\text{Se}_{0.30}\text{Te}_{0.70}$. In such Se-doped sample, the magnetism/structure instability is suppressed and superconductivity appears instead. Figure 4(a) shows the temperature dependence of resistivity ρ_{ab} on the single crystal $\text{Fe}_{1.03}\text{Se}_{0.30}\text{Te}_{0.70}$ with $I\parallel ab$ at zero field. ρ_{ab} increases with decreasing T and shows a sharp drop to zero at about 11 K, indicating a superconducting transition. The Hall coefficient R_H , as shown in the inset of Fig. 4(a), is positive, suggesting dominantly hole-type conducting carriers. Figures 4(b) and 4(c) show $\rho_{ab}(T)$ for $\text{Fe}_{1.03}\text{Se}_{0.30}\text{Te}_{0.70}$ in external magnetic fields up to 14 T within ab plane and along c axis, respectively. We can see that the superconducting transition is broadened slightly in magnetic fields up to 14 T. The behavior is rather different from polycrystalline LaOFeAs where the superconducting transition is broadened strongly in magnetic fields.²⁰ Fig. 4(d) shows $H_{c2}-T_c$ curves for both $H\parallel ab$ and $H\parallel c$, respectively, where T_c is defined by a criterion of 50% of normal state resistivity. The curves $H_{c2}(T)$ are very steep with slopes $dH_{c2}^{ab}/dT|_{T_c}=5.96$ T/K for $H\parallel ab$ and $dH_{c2}^c/dT|_{T_c}=3.69$ T/K for $H\parallel c$. Using the Werthamer-Helfand-Hohenberg formula²¹ $H_{c2}(0)=-0.69(dH_{c2}/dT)T_c$ and taking $T_c=12.4$ K, the upper critical fields are estimated as $H_{c2}^{ab}=51$ T and $H_{c2}^c=31$ T, respectively. It is important to note that those values are very large, comparable to the values found for F -doped LaFeAsO with T_c higher than 20 K.²⁰

It has been well known that, for the two-gap superconductivity in the dirty limit, the impurity scattering could strongly enhance the upper critical field H_{c2} .²² Such a trend is clearly observed for MgB_2 , a dirty two-gap superconductor, where the H_{c2} increases remarkably with the increase in resistivity by alloying MgB_2 with nonmagnetic impurities.²² Then, the very high H_{c2} observed in $\text{Fe}_{1.03}\text{Se}_{0.30}\text{Te}_{0.70}$ could be reasonably attributed to the strong impurity scattering effect from the randomly distributed excess Fe in such a new multiple band superconductor. The impurity scattering, particularly in the case of Fe^+ with a magnetic moment, would also suppress T_c . This could be the reason why T_c is not so high, although density-functional calculations indicated a higher strength of SDW order in stoichiometric FeTe , and therefore expected a higher T_c after the suppression of SDW order.^{6,11}

To conclude, the electronic properties of single-crystalline $\text{Fe}_{1.05}\text{Te}$ and $\text{Fe}_{1.03}\text{Se}_{0.30}\text{Te}_{0.70}$ were studied. The excess Fe

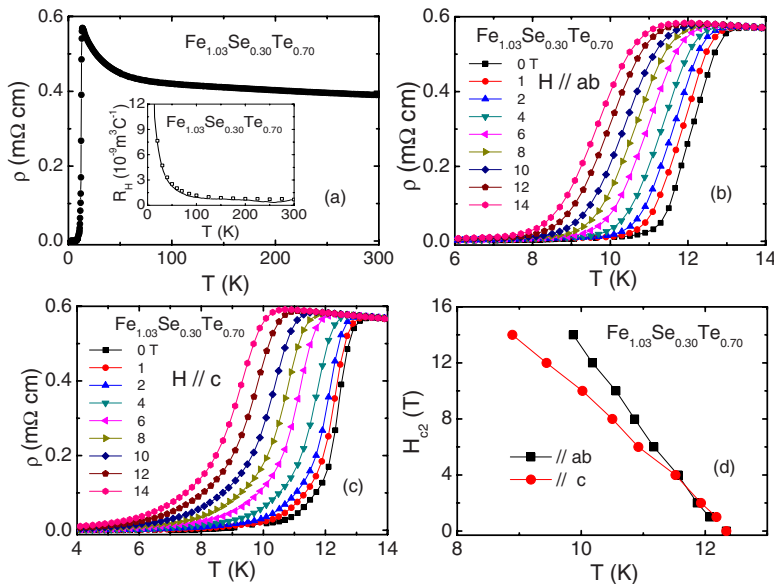


FIG. 4. (Color online) (a) Temperature dependence of the in-plane electrical resistivity for $\text{Fe}_{1.03}\text{Se}_{0.30}\text{Te}_{0.70}$ at zero field. Inset: temperature dependence of Hall coefficient for $\text{Fe}_{1.03}\text{Se}_{0.30}\text{Te}_{0.70}$. (b) and (c) Temperature dependence of the in-plane electrical resistivity for $\text{Fe}_{1.03}\text{Se}_{0.30}\text{Te}_{0.70}$ in low temperature region at fixed fields up to 14 T for $H \parallel ab$ plane and $H \parallel c$ axis, respectively. (d) $H_{c2}(T)$ plot for $H \parallel ab$ plane (closed square) and $H \parallel c$ axis (closed circle), respectively.

ions in those compounds dramatically modify their properties. For $\text{Fe}_{1.05}\text{Te}$ above T_{SDW} , we could not identify well-defined quasiparticles with sufficiently long lifetime. Below T_{SDW} , a small Drude component develops at low frequency due to the dramatic reduction in carrier scattering rate. But unlike LaFeAsO and SrFe_2As_2 , there is no clear sign of gap opening from optical, Hall coefficient and low- T specific-

heat measurement results. Strong impurity scattering effect seems to exist also in Se-doped superconducting sample, which leads to a relatively low T_c but a rather high upper critical field in such a new multiple band superconductor.

This work is supported by the NSFC, CAS, and the 973 project of the MOST of China.

- ¹Y. Kamihara, T. Watanabe, M. Hirano, and H. Hosono, *J. Am. Chem. Soc.* **130**, 3296 (2008).
- ²F. C. Hsu, T. Y. Luo, K. W. Yeh, T. K. Chen, T. W. Huang, Phillip M. Wu, Y. C. Lee, Y. L. Huang, Y. Y. Chu, D. C. Yan, and M. K. Wu, *Proc. Natl. Acad. Sci. U.S.A.* **105**, 14262 (2008).
- ³M. H. Fang, H. M. Pham, B. Qian, T. J. Liu, E. K. Vehstedt, Y. Liu, L. Spinu, and Z. Q. Mao, *Phys. Rev. B* **78**, 224503 (2008).
- ⁴K. W. Yeh, T. W. Huang, Y. L. Huang, T. K. Chen, F. C. Hsu, Phillip M. Wu, Y. C. Lee, Y. Y. Chu, C. L. Chen, J. Y. Luo, D. C. Yan, and M. K. Wu, *Europhys. Lett.* **84**, 37002 (2008).
- ⁵Y. Mizuguchi, F. Tomioka, S. Tsuda, T. Yamaguchi, and Y. Takanashi, *Appl. Phys. Lett.* **93**, 152505 (2008).
- ⁶A. Subedi, L. Zhang, D. J. Singh, and M. H. Du, *Phys. Rev. B* **78**, 134514 (2008).
- ⁷D. Fruchart and P. Convert P. Wolfers, R. Madar, J. P. Senateur, and R. Fruchart, *Mater. Res. Bull.* **10**, 169 (1975).
- ⁸W. Bao, Y. Qiu, Q. Huang, A. Green, P. Zajdel, M. R. Fitzsimmons, M. Zhernenkov, M. Fang, B. Qian, E. K. Vehstedt, J. Yang, H. M. Pham, L. Spinu, and Z. Q. Mao, arXiv:0809.2058 (unpublished).
- ⁹Shiliang Li, Clarina de la Cruz, Q. Huang, Y. Chen, J. W. Lynn, Jiangping Hu, Yi-Lin Huang, Fong-chi Hsu, Kuo-Wei Yeh, Maw-Kuen Wu, and Pengcheng Dai, *Phys. Rev. B* **79**, 054503 (2009).
- ¹⁰M. J. Pitcher, D. R. Parker, P. Adamson, S. J. C. Herkelrath, A. T. Boothroyd, R. M. Ibberson, M. Brunelli, and S. J. Clarke, *Chem. Commun.* (2008) 5918.
- ¹¹L. Zhang, D. J. Singh, and M. H. Du, *Phys. Rev. B* **79**, 012506 (2009).
- ¹²C. C. Homes, M. Reedyk, D. A. Crandles, and T. Timusk, *Appl. Opt.* **32**, 2976 (1993).
- ¹³G. F. Chen, Z. Li, J. Dong, G. Li, W. Z. Hu, X. D. Zhang, X. H. Song, P. Zheng, N. L. Wang, and J. L. Luo, *Phys. Rev. B* **78**, 224512 (2008).
- ¹⁴G. M. Zhang, Y. H. Su, Z. Y. Lu, Z. Y. Weng, D. H. Lee, and T. Xiang, arXiv:0809.3874 (unpublished), and references therein.
- ¹⁵C. Fang, H. Yao, W.-F. Tsai, J. P. Hu, and S. A. Kivelson, *Phys. Rev. B* **77**, 224509 (2008); C. Xu, M. Müller, and S. Sachdev, *ibid.* **78**, 020501(R) (2008).
- ¹⁶F. J. Ma, W. Ji, J. P. Hu, Z. Y. Lu, and T. Xiang, arXiv:0809.4732 (unpublished).
- ¹⁷J. Dong, H. J. Zhang, G. Xu, Z. Li, G. Li, W. Z. Hu, D. Wu, G. F. Chen, X. Dai, J. L. Luo, Z. Fang, and N. L. Wang, *Europhys. Lett.* **83**, 27006 (2008).
- ¹⁸W. Z. Hu, J. Dong, G. Li, Z. Li, P. Zheng, G. F. Chen, J. L. Luo, and N. L. Wang, *Phys. Rev. Lett.* **101**, 257005 (2008).
- ¹⁹C. Fang, B. A. Bernevig, and J. P. Hu, arXiv:0811.1294 (unpublished).
- ²⁰G. F. Chen, Z. Li, G. Li, J. Zhou, D. Wu, J. Dong, W. Z. Hu, P. Zheng, Z. J. Chen, H. Q. Yuan, J. Singleton, J. L. Luo, and N. L. Wang, *Phys. Rev. Lett.* **101**, 057007 (2008).
- ²¹N. R. Werthamer, E. Helfand, and P. C. Hohenberg, *Phys. Rev.* **147**, 295 (1966).
- ²²A. Gurevich, S. Patnaik, V. Braccini, K. H. Kim, C. Mielke, X. Song, L. D. Cooley, S. D. Bu, D. M. Kim, J. H. Choi, L. J. Belenky, J. Giencke, M. K. Lee, W. Tian, X. Q. Pan, A. Siri, E. E. Hellstrom, C. B. Eom, and D. C. Larbalestier, *Supercond. Sci. Technol.* **17**, 278 (2004).